



RESEARCH ARTICLE

ADSORPTION OF TEXTILE DYE ACID GREEN 42 (AG42) ON ACTIVATED CARBON FROM CHICKEN EGGSHELLS (CAC30)

Djibiliour Sanogo¹, Gouegoui Serge Pacôme Bohui¹ and Ladji Méité²

1. Department of Physics Chemistry, Felix Houphouet-Boigny University, Abidjan, Côte d'Ivoire.
2. Department of Environmental Sciences, Nangui Abrogoua University, Abidjan, Côte d'Ivoire.

Manuscript Info

Manuscript History

Received: 10 July 2024

Final Accepted: 14 August 2024

Published: September 2024

Key words: -

Adsorption, Chicken Eggshells, Activated Carbon, Acid Green 42

Abstract

The present work is a contribution to the valorization of chicken eggshells, an abundant waste product in Côte d'Ivoire, as a credible alternative to commercial activated carbon. Chemical activation of the precursor was carried out with 30% phosphoric acid for 24 h of contact in a ratio of 200 g of material to 100 mL of acid, and calcined at 600°C for 1h. The surface of the activated carbon obtained was studied using the BET (Brunauer-Emmett and Teller) method, which consists in establishing the adsorption isotherm for nitrogen N₂. The results reveal a specific surface area of 5.42 m². g⁻¹, 65.68% of micropores and a pH_{zpc} of 7.40. Chemical characteristics determined by Boehm's method indicate the basic nature of the surface. The elemental composition is dominated by oxygen (50.53%), calcium (30.78%) and carbon (11.33%). The experiments demonstrated that the removal of AG42 by adsorption on CAC30 is influenced by contact time, activated carbon mass, solution pH, and initial concentration and temperature of the dye aqueous solution. Adsorption kinetics followed the pseudo-second-order model and the isotherm is described by the Langmuir model. The thermodynamic study revealed the spontaneous ($\Delta G < 0$) and exothermic ($\Delta H < 0$) nature of dye adsorption, with a well-organized distribution of dye molecules at the adsorption sites ($\Delta S^\circ < 0$).

Copyright, IJAR, 2024, All rights reserved.

Introduction: -

The recovery of waste, especially of agricultural origin, is an important part of its sustainable management and fits perfectly into the circular economy process. This management is fundamental to the preservation of the environment and human health [1]. Among the dangers threatening the environment and health, textile dyes pose a particular threat due to the properties of these molecules [2]. Indeed, with the development of dyeing units, particularly small-scale ones, these substances are discharged daily into surface waters via sewage networks. However, these compounds, which are difficult to biodegrade, are known to be toxic or harmful to humans and animals [3]. Maurya et al. and Vanessa et al [4,5] have reported that organic dyes are responsible for a number of deleterious effects on human health; some dyes are carcinogenic, mutagenic and teratogenic, and may cause a number of ailments. The reduction, or even elimination, of these dyes is therefore necessary: Several treatment techniques based on laboratory and industrial scales were developed for dyes removal from wastewaters [6]. They include physico-chemical processes (adsorption, membrane filtration, solid-liquid separation methods: precipitation, coagulation, flocculation and decantation), chemical processes (ion exchange resins, oxidation by: oxygen, ozone, advanced oxidation processes...) and biological processes (aerobic and anaerobic treatment) [7]. Among these technologies, adsorption offers considerable advantages in terms of

Corresponding Author: - Djibiliour Sanogo

Address: - Department of Physics Chemistry, Felix Houphouet-Boigny University, Abidjan, Côte d'Ivoire.

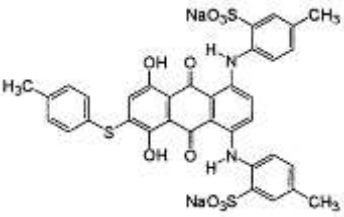
simplicity of implementation, flexibility and the absence of harmful by-products [8]. However, commercial activated carbon, the adsorbent par excellence for this technique, remains inaccessible, particularly for developing countries, due to its high cost [9]. It is in this context that our work focuses on the use of chicken eggshells, abundant in Côte d'Ivoire, as activated carbon for the removal of the textile dye Acid Green 42 (AG42), an anthraquinone dye, in aqueous media.

Materials and Methods:

Reagents and solvents

The Acid Green 42 (AG42) dye (Table I) of 100% purity was supplied by Cypress Diagnostics. Phosphoric acid (H_3PO_4), sodium hydroxide (NaOH) (99.9%), sodium chloride (NaCl) (99%), sodium carbonate (Na_2CO_3) (99%), sodium hydrogen carbonate (NaHCO_3), hydrochloric acid (0.1 N) (HCl), sodium thiosulfate solution ($\text{Na}_2\text{S}_2\text{O}_3$) (85-100%) and iodine (I_2) (85%) were supplied by Scharlab SL. Solutions were prepared using deionized water.

Table I: - Characteristics of Acid Green 42 textile dye [10].

Usual name	Acid Green 42
Structure and chemical name	Alizarin cyanine green 3GW 
Molecular formula	$\text{C}_{35}\text{H}_{26}\text{N}_2\text{Na}_2\text{O}_8\text{S}_3$
Cas number	6425-06-5
Molecular mass	744,77 $\text{g}\cdot\text{mol}^{-1}$
Solubility	High solubility in water and alcohol
Purity	99,5%

Preparation of activated carbon (CAC30):

Hen eggshells, collected from markets in Abidjan (southern Côte d'Ivoire), were washed in hot water and dried to remove oil residues and impurities before being ground in a Romer Labs-type grinder, washed with distilled water and oven-dried at 110°C for 24 hours. The crushed material was sieved using an electric sieve shaker (RETSCH-AS200). The crushed material was cold-impregnated for 24 hours in a 30% solution of phosphoric acid (H_3PO_4) at a ratio of 200 g to 100 mL acid. The impregnate is then dewatered and oven-dried for 24 hours at 110°C before being calcined at 600°C in a muffle furnace (NABERTHERM) for 1 hour. After cooling, the activated carbon is washed several times with distilled water to remove the activating agent, then dried in an oven at 110°C for 24 hours. The fraction between 1 and 2 mm was selected for the AG42 dye removal tests.

Preparation of AG42 solutions:

The AG42 stock solution of 1 g/L was prepared by dissolving 1 g of powder in 1 liter of distilled water heated to boiling temperature (100°C). Daughter solutions for analysis were obtained by successive dilutions of the stock solution for adsorption tests. The adsorption spectrum of the solution, measured between 400 and 800 nm, was used to determine the molecule's maximum adsorption wavelength (578nm). A dye calibration curve was established to determine residual concentrations during adsorption tests on the prepared carbon.

Characterization of the activated carbon obtained

Iodine value: The iodine value was determined using the experimental protocol proposed by Rager and al [11]. A 0.2 g mass of activated carbon was brought into contact with 20 mL of a 0.02 N iodine solution, then shaken for 5 min. After filtration, 10 mL of the filtrate is withdrawn and titrated with sodium thiosulfate solution ($\text{Na}_2\text{S}_2\text{O}_3$) until discoloration. From the equation for the reaction of iodine with sodium thiosulfate, we deduce the expression for the amount of iodine adsorbed by the activated carbon. The iodine value expressed in mg/g is given by relationship 1.

$$\text{Iodine value} \left(\frac{\text{mg}}{\text{g}} \right) = \frac{\left[C_0 - \frac{C_n \times V_n}{2V_{I_2}} \right] \times M_{I_2} \times V_{\text{ads}}}{m} \quad (1)$$

where C_0 and C_n are the initial concentration of iodine (mol.L^{-1}) and that of the sodium thiosulfate solution (mol.L^{-1}), respectively; V_n , V_{I_2} and V_{ads} are the volumes of the sodium thiosulfate solution at equivalence (mL) and that of the iodine solution dosed (10mL), respectively; M_{I_2} is the molecular weight of iodine (254 g/mol) and m the mass of activated carbon (g).

Surface functions:

Measurements are carried out using the Boehm method [12] described by Khalifaoui and al [13] as follows: 1g of dry activated carbon is brought into contact with 50 mL each of 0.1 N aqueous solutions of NaOH, Na_2CO_3 , NaHCO_3 and HCl. Each solution is stirred for 24 hours to ensure that as many surface groups as possible have reacted. After filtration, 10 mL of each solution is assayed acid-base. The basic solutions are assayed with 0.1 M hydrochloric acid and the acid solution with 0.1 N sodium hydroxide.

Zero charge pH (pH_{ZC}):

The pH_{ZC} is determined using the technique reported by Kifuani and al [14]. The pH derivative method involves placing 50 mL of 0.01 M NaCl solutions in closed vials and adjusting the pH of each (2, 4, 6, 8, 10 and 12) by adding 0.1 M NaOH or HCl solution. 0.15 g of activated carbon is then added to each flask. The suspensions are kept under agitation at room temperature for 24h, after which the final pH is determined. The pH_{ZC} is the point at which the curve pH_{final} versus $\text{pH}_{\text{initial}}$ intercepts the line $\text{pH}_{\text{final}} = \text{pH}_{\text{initial}}$.

BET specific surface area:

The method proposed by Brunauer, Emmet and Teller is based on the adsorption of nitrogen at a temperature of 77K on activated carbon, enabling its specific surface area to be determined [15]. The BET equation used in practice in its linear form is given by relation 2.

$$\left(\frac{P/P_0}{Q_{\text{ads}}(1 - P/P_0)} \right) = \frac{1}{Q_m C} + \frac{(C-1)}{Q_m C} \times \frac{P}{P_0} \quad (2)$$

Where Q is the quantity adsorbed at pressure P , Q_m the quantity of gas required to cover 1g of adsorbent with a single layer of gas and C the BET.

The plot of $\frac{(P/P_0)}{Q_{\text{ads}}(1 - P/P_0)}$ as a function of P/P_0 is a straight line with slope $a = \frac{(C-1)}{Q_m C}$ and y intercept $b = \frac{1}{Q_m C}$ which allow us to determine the constants $Q_m = \frac{1}{a+b}$ and $C = 1 + \frac{a}{b}$. The specific surface area S_{BET} is calculated from equation 3.

$$S_{\text{BET}} = \sigma N Q \quad (3)$$

Where P is the partial pressure, P_0 is the saturation vapour pressure of the adsorbate at the temperature of measurement, σ is the surface area occupied by a vapour molecule (at $T=77\text{K}$, the surface area of a nitrogen molecule is $\sigma = 16.2 \text{ \AA}^2 = 16.2 \cdot 10^{-20} \text{ m}^2$) and N is Avogadro's number ($6.025 \cdot 10^{23} \text{ mol}^{-1}$).

t-plot method:

The t-plot method, used in conjunction with the BET method, can be used to determine the value of the microporous surface of carbon [10]. Thus, from the number of molecular layers adsorbed at pressure P on the solid given by the ratio between the volume V of vapor adsorbed at each pressure P and the value V_m of the monolayer volume calculated by the BET equation, the thickness was determined with e as the statistical thickness of amino-molecular layer by relation 4.

$$t = \frac{V}{V_m} e = e \frac{P_0}{(P_0 - P)} \quad (4)$$

Elemental composition

Following the protocol of Habeeb et al [16], 100 mg of charcoal were used for these analyses. The main elements determined were oxygen (O), carbon (C) and hydrogen (H) content, as well as exchangeable ions such as calcium (Ca^{2+}), sodium (Na^+), potassium (K^+) and magnesium (Mg^{2+}). The samples were deposited on a surface called a plot, 12 cm in diameter. After placement on the pad, the sample sare metallized with at hinlayer of gold using the Q150-RS metallizer. This step makes the charcoal layer conductive and prevents the sample from igniting during analysis. The analys is was carried out at PETROCI's analys is and research center in Abidjan.The equipment used is a FEG Supra VP Zeiss scanning electron microscope (SEM) coupled to an EDS (Energy Diffusion Spectrometry) X-ray micro analyzer. It provides information on sample chemical composition and pore morphology.

AG42 textile dye removal tests

In order to determine the optimum conditions for using the activated carbon obtained, the influence of certain parameters was studied, notably contact time, carbon dose, pH of the AG42 solution, initial concentration and solution temperature.

Influence of contact time:

To study the influence of contact time on adsorption kinetics, a 10 g mass of CAC30 is brought into contact with 1 L of AG42 at a concentration of 100 mg/L.

Influence of activated carbon dose:

The optimum mass of CAC30 is determined by contacting different masses of carbon (10 g/L, 20 g/L, 30 g/L, 40 g/L and 50 g/L) with 1 L of 100 mg/L solution.

Influence of AG42 solution pH:

100 mg/L solutions of AG42 at different pH levels were prepared. The pH was adjusted to the desired value using hydrochloric acid solutions or 0.1 N sodium hydroxide. In an Erlenmeyer flask, the carbon dose was brought into contact with 1 L of the 100 mg/L colored solution. pH values range from 2 to 10 (2; 4; 6; 8; 10).

Influence of AG42 solution concentration:

To determine the influence of residue concentration on adsorption, the optimum dose of CAC30 is contacted with different concentrations of AG42 (25, 50, 100, 150 and 200 mg/L) at room temperature.

Influence of AG42 solution temperature:

To determine the influence of temperature on dye adsorption, the optimum dose of CAC30 is brought into contact with 1 L of dye of optimum concentration in an Erlenmeyer flask. The flask is tightly sealed and placed in a thermostated bath at various temperatures (30°C, 35°C, 40°C, 45°C and 50°C).

Determination of adsorption rate:

Solutions are stirred on a magnetic stirrer at 300 rpm for 3 hours. Samples are taken at intervals, and the suspensions obtained after centrifugation are analyzed for residual concentrations using a Visible Spectrophotometer. The setests are used to determine the adsorption rate and quantity of AG42.

$$\text{Adsorptionrate}(\%) = \frac{(C_i - C_t)}{C_i} \times 100 \quad (5)$$

$$Q_t = (C_i - C_t) \times V / m \quad (6)$$

Modeling the adsorption kinetics and isotherm of AG42 on CAC30 kinetic models used to describe adsorption in static mode. Static-mode adsorption data for AG42 on CAC30 were analyzed on the basis of three kinetic models widely used in the literature: the pseudo-first-order, pseudo-second-order and intra-particle diffusion models. The models are expressed respectively by the following equations:

$$\ln(Q_e - Q_t) = \ln Q_e - k_1 t \quad (7)$$

Q_t is the amount of AG42 adsorbed (mg/g) at time t , Q_e is the equilibrium adsorption capacity, and k_1 is the rate constant (min^{-1}).

$$\frac{1}{Q_t} = \frac{1}{K_2 Q_e^2 t} + \frac{1}{Q_e} \quad (8)$$

K_2 is the second-order rate constant (g/min.mg).

$$Q_t = K_i \times t^{0.5} + C \quad (9)$$

K_i is the intra-particle diffusion constant (mg.g⁻¹.hour^{-0.5}), C , a constant (mg.g⁻¹) and Q_t , the amount of AG42 fixed by the adsorbent at time t (mg.g⁻¹).

The three equations were used to determine the kinetic parameters of the three models.

Mathematical models used to describe adsorption isotherms

Numerous theoretical models have been developed to describe adsorption isotherms. However, we are interested in three models commonly used to describe the adsorption isotherm on activated carbon. These are the Langmuir, Freundlich and Temkin models. These models are represented respectively by the following equations:

$$Q_e = \frac{Q_m b C_e}{1 + b C_e} \quad (10)$$

Q_e is the quantity of adsorbate fixed at equilibrium by the adsorbent (mg.g⁻¹), C_e is the residual concentration at equilibrium (mg.L⁻¹), Q_m is the maximum saturation quantity of the adsorbent (mg.g⁻¹) and b is the thermodynamic constant of the adsorption equilibrium (L.mg⁻¹).

$$\ln(Q_e) = \ln K_F + \frac{1}{n} \ln(C_e) \quad (11)$$

C_e is the concentration of the AG42 solution at equilibrium (mg/L), Q_e the adsorption capacity of the adsorbents at equilibrium (mg/g), K_F and n are the Freundlich constants, indicative of adsorption capacity and intensity respectively.

$$\ln C_e = \frac{Q_e}{RT} b_T - \ln(K_T) \quad (12)$$

K_T and b_T represent the parameters of this model. K_T is the equilibrium constant (L.mg⁻¹), b_T is the adsorption energy change (J.mol⁻¹), R is the perfect gas constant (8.314 J.mol⁻¹.K⁻¹) and T is the absolute temperature (K).

Thermodynamic parameters:

This study determines thermodynamic parameters such as standard enthalpy (ΔH°), standard entropy (ΔS°) and standard free enthalpy (ΔG°). Experimentally, these parameters are determined using equations 13, 14 and 15 [17].

$$\ln K_d = \frac{\Delta S^\circ}{R} - \frac{\Delta H^\circ}{RT} \quad (13)$$

$$K_d = \frac{V}{m} \frac{C_o - C_e}{C_e} \quad (14)$$

$$\Delta G^\circ = \Delta H^\circ - T\Delta S^\circ \quad (15)$$

K_d is the distribution coefficient (mL.g⁻¹), R is the perfect gas constant ($R=8.314$ J.mol⁻¹.K⁻¹) and T is the absolute temperature (K). The values of ΔH° and ΔS° are obtained by plotting $\ln(K_d)$ versus $1/T$.

Results and Discussion:-

Characterization of prepared activated carbon

Elemental composition and surface topography:

Pore topography and elemental composition of CAC30 was carried out at PETROCI's Abidjan/Côte d'Ivoire Analysis and Research Center in the SEM/EDS department. Figure 1 and Table II show the main results.

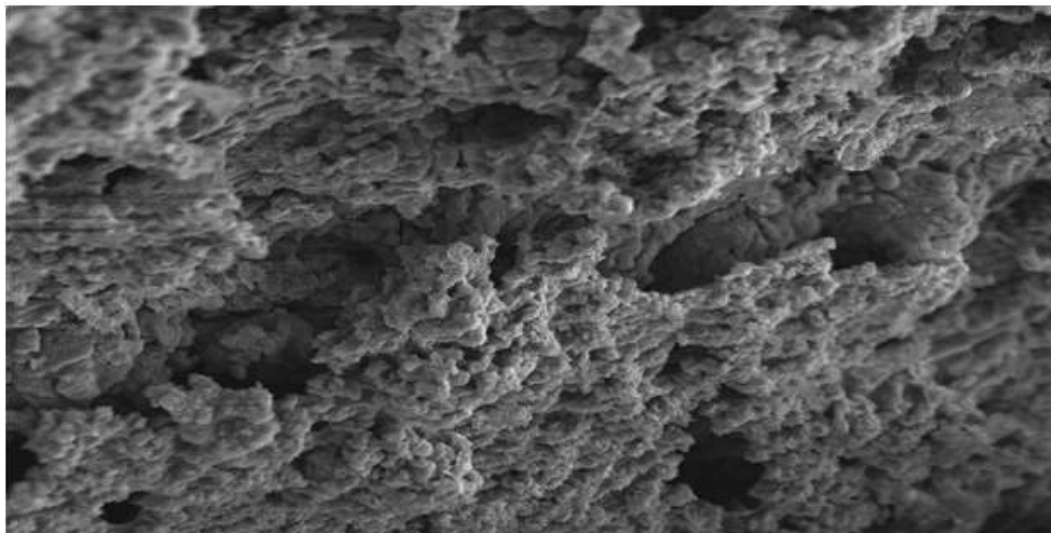


Figure 1: -SEM image of the CAC30 surface.

CAC30 has a very undeveloped surface with very few pores. Hen eggshells with a crystalline structure remain very poorly developed during the impregnation and calcination stages. These results are in agreement with those of Habeeb and al [16].

Tableau I:-Elemental composition of the activated carbons prepared (% by mass)

Elt	C	Mg	P	Ca	Sc	Te	Pt	O	Total
CAC30	11,33	0,20	5,39	30,78	0,28	1,16	0,75	50,53	100,00

These results also show that CAC30 consists essentially of carbon (11.33%), phosphorus (5.39%), calcium (30.78%) and oxygen (50.53%). Similar results were reported by Habeeb and al [16] in their studies. These authors reported carbon contents ranging from 2.56 to 24.36%, oxygen from 53.99 to 65.03% and calcium from 12.48 to 39.15%.

Surface function:

The Boehm surface function assay was used to quantify the surface functional groups of CAC30. The results are shown in Table III. They show at total acidity of 3.21 meq/g and at total basicity of 4.96 meq/g. The acidity is mainly due to carboxylic functions (1.53 meq/g) and phenolic functions (1.64 meq/g).

Table III: - Surface chemical characteristics of CAC30.

Carboxylic (meq/g)	Phenolic (meq/g)	Lactonic (meq/g)	Totalacid (meq/g)	Totalbasic (meq/g)	Character	pHzc
1,53	1,64	0,04	3,21	4,96	Basic	7,40

CAC30 has both acidic and basic functions, suggesting that it can adsorb both anionic and cationic dyes. According to Mezerette and Vergnet [18], the surface functions of activated carbon may originate from activation processes. They could also be born of bonds between oxygen and the various atoms present in the precursor material: hydrogen, chlorine, sulfur, nitrogen, etc. Several authors, including Crini and Bardot [19], support this assertion. The presence of both acidic and basic functional groups, with basic dominance, could explain the pHzc value of 7.40.

Specific surface area and iodine value

The results of the nitrogen (N_2) adsorption and desorption isotherms at 77 K, the plot of the BET equation transform and the surface area distribution as a function of pore diameter for CAC30 are shown in Figures 2, 3, 4 and 5

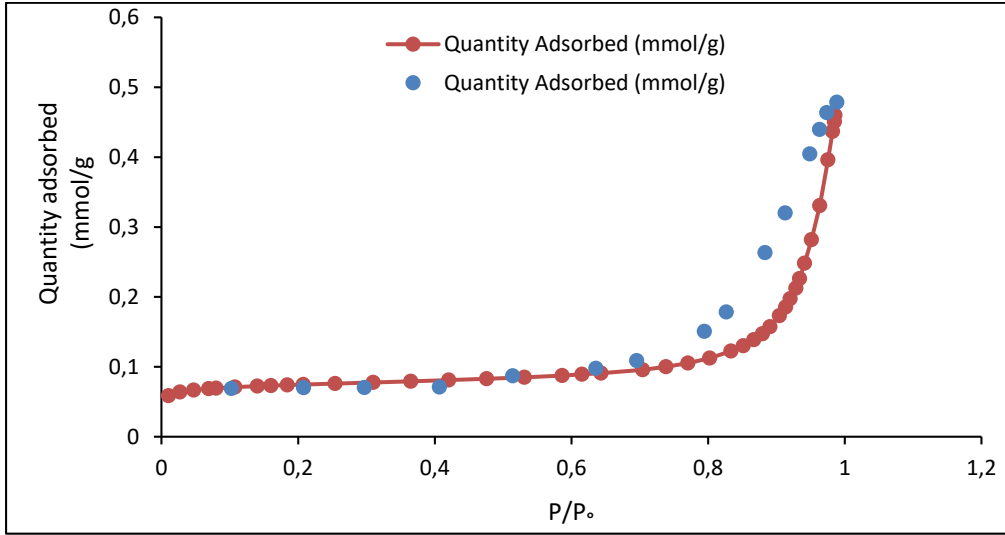


Figure 2: -Adsorption and desorption isotherms for N₂ on CAC30.

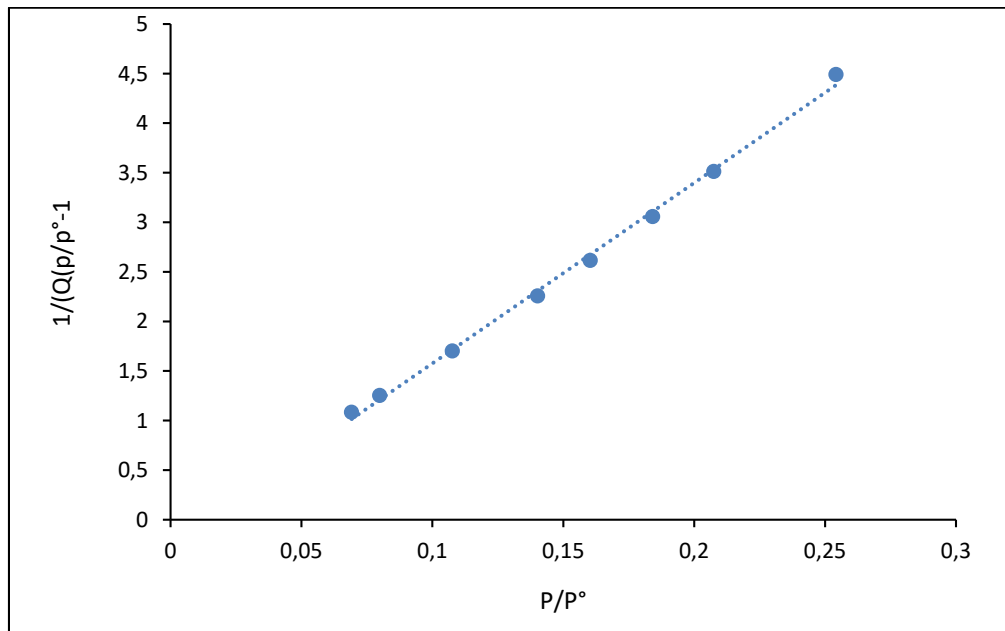


Figure 3: -BET equation transform plots for CAC30.

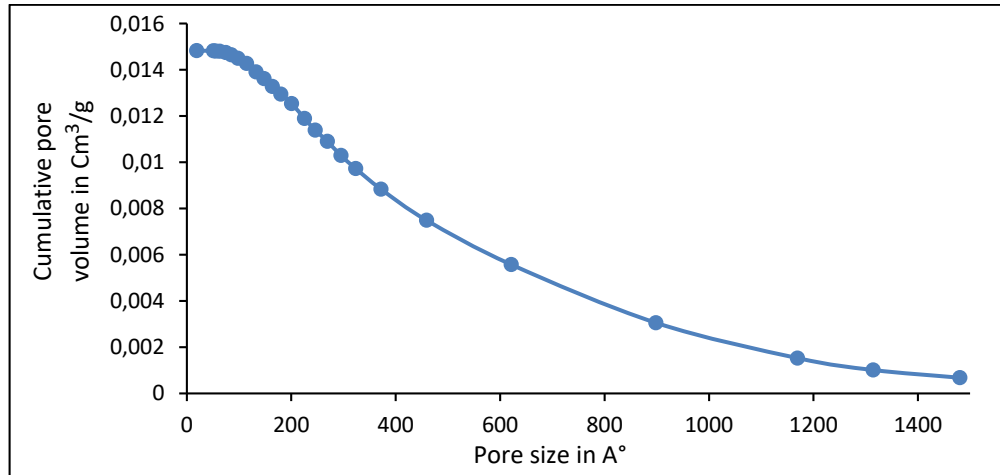


Figure 4: -Volume area distribution as a function of pore diameter.

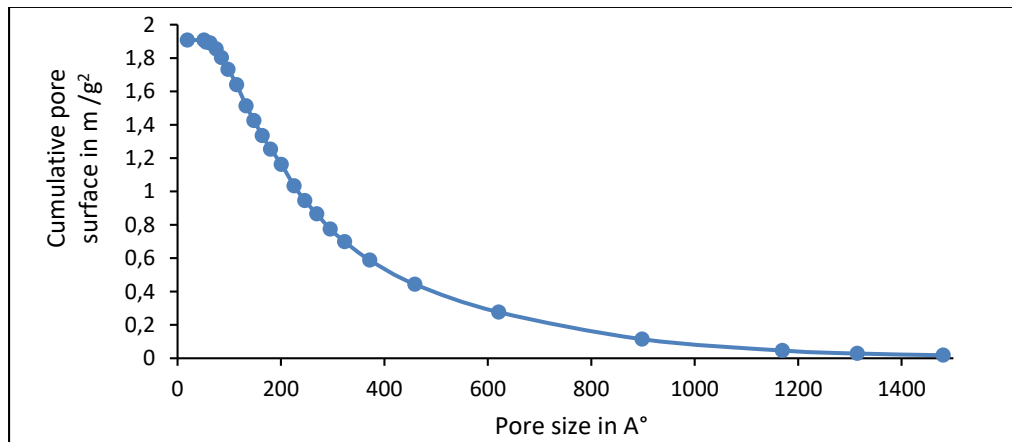


Figure 5: -Surface area distribution as a function of pore diameter.

The shape of the curve (Figure 2) indicates that the adsorption isotherm for nitrogen on CAC30 is of type I (Langmuir isotherm) according to the IUPAC classification. This type of isotherm suggests that the adsorbent is microporous. The speed at which the plateau is reached is an indication of the pore size distribution, and the presence of the horizontal plateau suggests a very low external surface area [20]. The adsorption isotherm gives access to the specific surface area, calculated using the BET method by extrapolation from the straight line in figure 3. Pore size distribution is calculated using the Barret, Joyner and Helenda (BJH) technique [21]. Figures 4 and 5 show the respective distribution of pore surface and pore volume as a function of pore size. Both curves show that surface area and volume are predominantly microporous. Nitrogen adsorption isotherms (N_2) also provide information on pore area, volume and actual pore diameter. Table IV summarizes the textural parameters of CAC30: BET surface area (S_{BET} m^2/g), microporous surface area (m^2/g), external surface area (S_{ext} m^2/g), total pore volume (V_{tot} cm^3/g) and iodine value.

Table IV: -Porosity of CAC30.

Total surface area S_{BET} ($m^2.g^{-1}$)	BET	5,429
Microporous surface area ($m^2.g^{-1}$)	(t-Plot)	3,565
External surface area S_{ext} ($m^2.g^{-1}$)	(t-Plot)	1,863
Total pore volume ($cm^3.g^{-1}$)	(t-Plot)	0,009
Iodine index ($mg.g^{-1}$)	Iodometry	450,85

BET analysis of CAC30 reveals a surface area of $5.429 \text{ m}^2/\text{g}$, dominated by micropores ($3.5659 \text{ m}^2/\text{g}$ or 65.68%). This low surface area is due to the structure of the precursor. Since eggshells have a crystalline structure, they don't react with phosphoric acid in the same way as lignocellulosic structures. In fact, during impregnation, a slight loss of mass was observed, reflecting the limited development of pores [22]. These authors reported similar surfaces for the same precursor. The iodine value of $450.85 \text{ m}^2/\text{g}$ could be due to the porous structure of chicken eggshells, which contain a large number of micropores, according to El-Kady and al [23], each eggshell contains between 7,000 and 17,000 pores. However, these micropores are very poorly developed during impregnation and calcination, which could explain the low surface values.

Optimization of AG42 adsorption on CAC30 activated carbon in static mode
 Study of the influence of contact time
 Tests were carried out on a 1 L solution at 100 mg/L and 10 g CAC30 mass. Figure 6 shows the evolution of the adsorption rate of AG42 on carbons as a function of time.

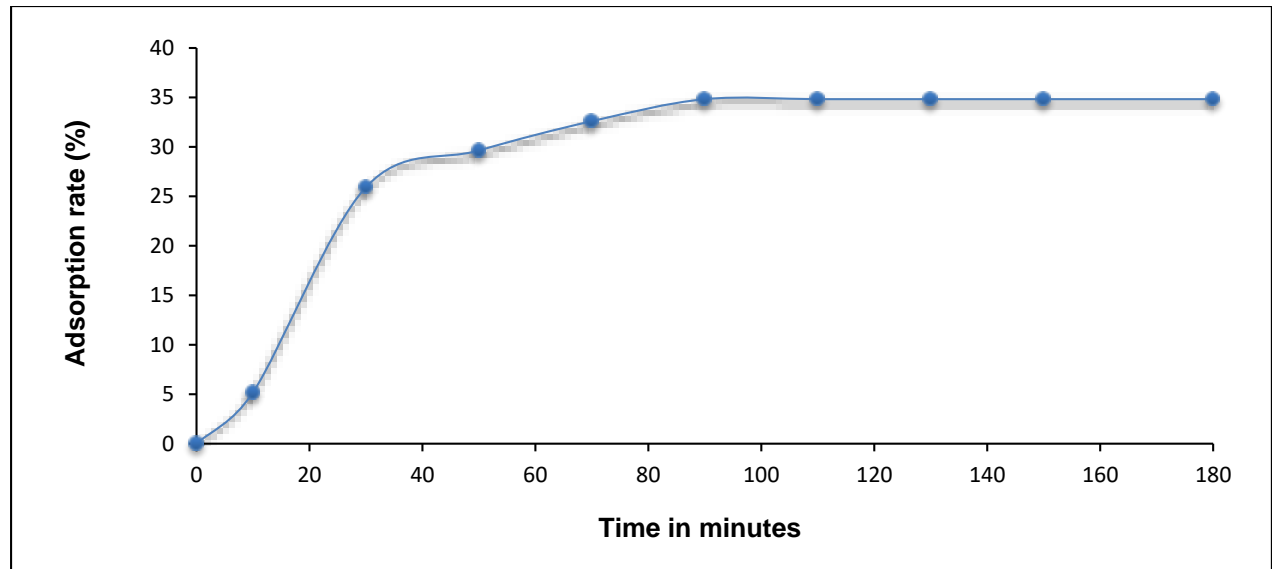


Figure 6:-Influence of contact time on AG42 adsorption.

Analysis of figure 6 reveals three parts: the first is characterized by rapid adsorption after 30 min, with removal efficiencies rising from 0 to 25.92%. This growth is thought to be due to the availability of free adsorption sites on the carbon surface. In this second part, the adsorption rate increases slowly with time. The plateau at 90 min indicates saturation of the available adsorption sites. The ultimate adsorption capacity (Q_m) of coals is thus reached. This same kinetic behavior has been reported in several studies [24, 25].

Study of the influence of adsorbent dose

Tests were carried out with carbon masses ranging from 10 to 50 g of CAC30 in 1 L of 100 mg/L solution. Figure 7 shows the evolution of the dye removal rate with the quantity of carbon introduced.

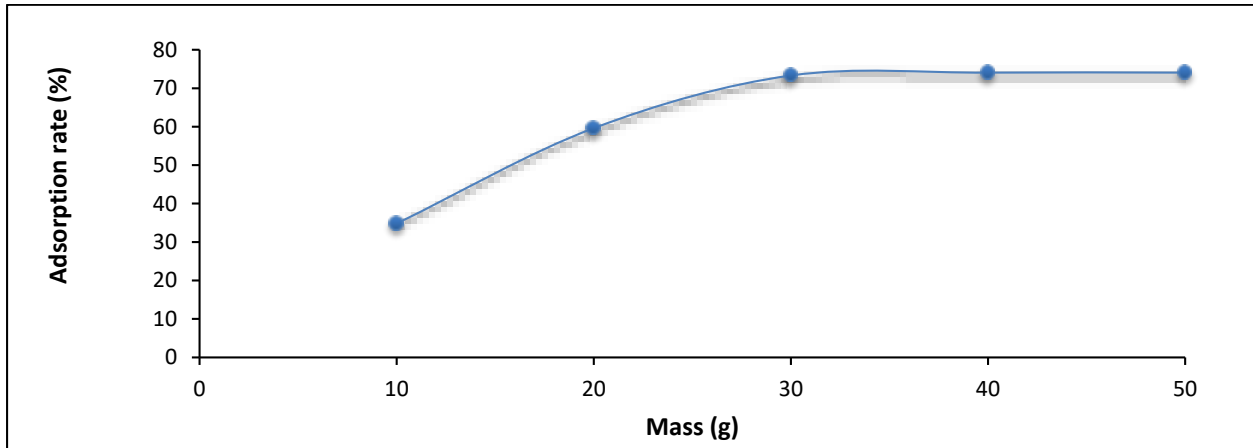


Figure 7: - Influence of activated carbon dose on AG42 removal.

The results presented in Figure 7 show an increase in the adsorption rate with increasing carbon mass. The adsorption rate rises from 34.81 to 74.07% when the masses are increased from 10 to 30 g respectively. From 30 g CAC30 onwards, the adsorption rate remains virtually constant despite the increase in CAC30 mass. The increase in adsorption rate observed with increasing charcoal mass could be attributed to the number of free sites increasing with the amount of charcoal up to the optimum mass. Above this mass, the addition of carbon would lead to the formation of agglomerates of carbon particles, excluding certain adsorption sites. Steric hindrance would therefore be at the root of the reduction in total surface area and adsorption capacity. This finding is reinforced by Sakr and al [26], who argue that low carbon concentrations make access to binding sites easier.

Study of the influence of the pH of the AG42 solution

Samples were prepared under the same operating conditions as above. The pH was adjusted to the desired value using hydrochloric acid or sodium hydroxide. Figure 8 shows the results

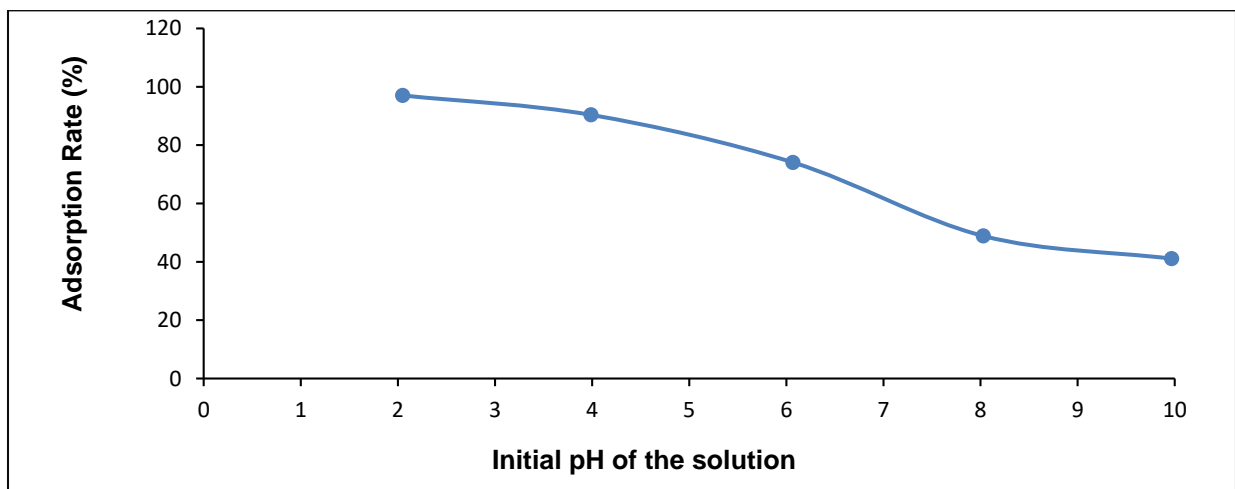


Figure 8: - Influence of the pH of the AG42 solution.

Examination of the influence of initial pH on adsorption of AG42 (Figure 8) shows that the rate of elimination decreases with increasing initial solution pH. It decreases from 97.03 to 41.11% as the pH increases from 2 to 10. The high elimination rate under acidic conditions could be explained by the interactions and availability of sites for anionic dye binding on the surface of this activated carbon. Indeed, in acidic media, the number of positively charged active sites intensifies, inducing a strong electrostatic attraction between the negatively charged dye and the positively charged surface [27]. Guendouz [28] obtained similar results when removing Cibacron Green from dry lentil biomass. The lower

adsorption rate in alkaline media could be explained by the high concentration and mobility of OH⁻ ions, which favours their adsorption to the detriment of the anionic dye [29].

Study of the influence of the concentration of the AG42 solution

Experiments were carried out with varying dye concentrations (25, 50, 100, 150 and 200 mg/L). The results are shown in Figure 9.

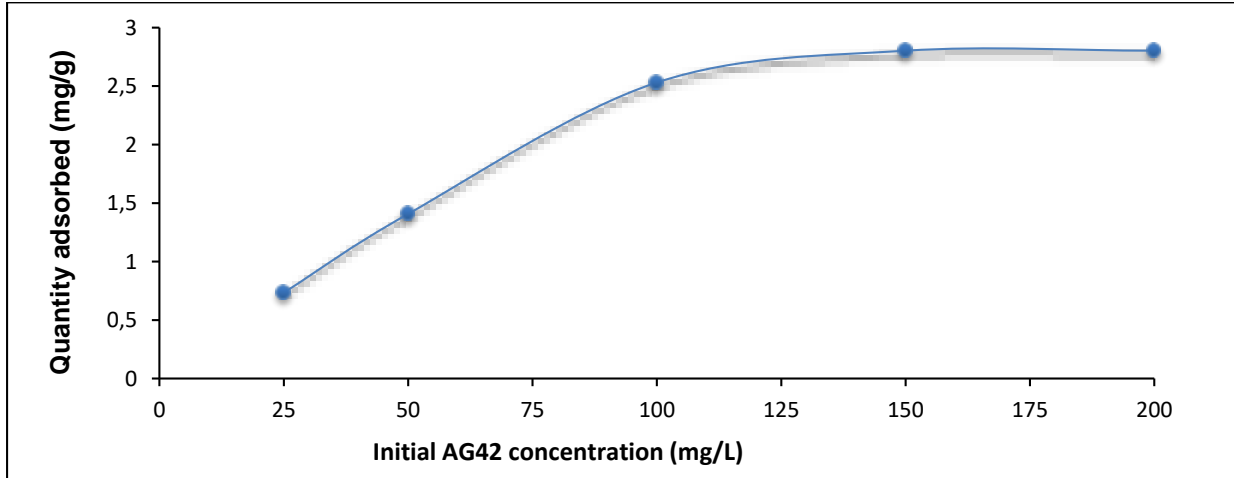


Figure 9: - Influence of the initial concentration of the AG42 solution.

The results in Figure 9 show that the amount of dye adsorbed increases with the concentration of AG42. This could be explained, by the ratio of the number of active sites on the carbon surface to the number of dye molecules in solution. Indeed, at low concentrations this ratio is high, leaving sites still unoccupied at equilibrium. These sites can be occupied when the initial concentration increases, due to the driving force that increases with concentration, facilitating the passage of solute from solution to the active sites. These results are in line with those obtained by several authors [30, 31, 32, 33].

Study of the influence of AG42 solution temperature

The influence of temperature was studied at the pH of the AG42 solution (6.20), immersed in a thermostated water bath to keep the desired temperature constant. The temperatures studied were 30, 35, 40, 45 and 50°C. Figure 10 shows the influence of temperature on dye retention capacity on CAC30.

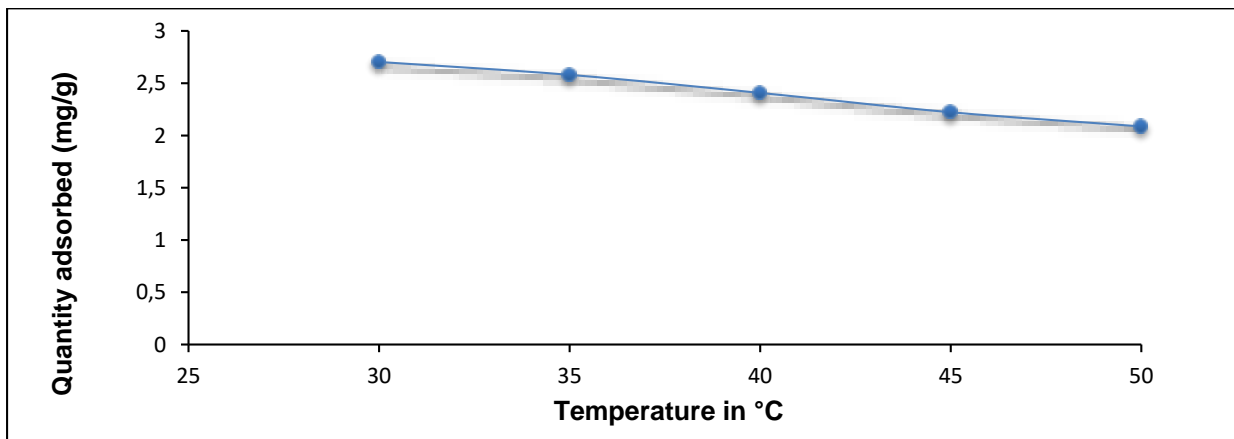


Figure 10:-Influence of temperature on AG42 adsorption.

This figure shows that the amount of dye adsorbed decreases with increasing reactor temperature. This decrease in the adsorption capacity of CAC30 could be explained by an increase in the number of collisions favoring desorption of molecules attached to the active sites. Similar results have been reported in several works, such as that on the binding of Congo Red (an anionic dye) to macete reed roots [34] and that of indigo carmine, or Acid Blue74, to de-oiled mustard waste [35], and showed a slight decrease as temperature increased.

Modeling adsorption kinetics

By modeling the adsorption kinetics, we can determine the corresponding characteristic constants (Table V) and check the correlation between experimental values and those predicted by the selected model.

TableV: -Kinetic model constants for the AG42/CAC30 system.

Adsorbent		CAC30				
Co (mg/L)		25	50	100	150	200
Qexp (mg/g)		0,73	1,41	2,53	2,80	2,82
Pseudo-first-order kinetics	Qe cal (mg/g)	0,88	0,96	2,24	1,91	2,13
	K1	-0,18	-0,11	-0,05	-0,10	-0,13
	R ²	0,89	0,91	0,89	0,90	0,75
Pseudo-second-order kinetics	Qe cal (mg/g)	0,74	1,44	2,85	2,89	2,91
	K2 (g/mg.min)	1,19	0,16	0,017	0,065	0,068
	R ²	0,99	0,99	0,99	0,99	0,99
Intra-particle diffusion kinetics	Qe cal (mg/g)	0,99	0,49	1,09	0,99	0,96
	Kint (g/mg.min)	0,18	0,09	0,20	0,18	0,17
	R ²	0,75	0,74	0,90	0,77	0,70

These results show that the equilibrium adsorbed quantity Q_e increases with increasing initial concentration. More over, the values of R^2 are very high, all equal to 0.99, and far exceed those obtained with the pseudo-first-order model. The theoretical quantities set at equilibrium Q_e are very close to the values found experimentally, in contrast to the pseudo-first-order and intra-particle diffusion models. These last two findings indicate that the adsorption process follows the pseudo-second-order model. Several authors have used this model to better represent adsorption kinetics on activated carbons [36, 37, 38].

Modeling adsorption isotherms

The adsorption isotherm indicate show the molecules are distributed between the solute and the carbon surface at equilibrium. Modeling adsorption isotherms is the first objective in any scientific investigation, since it enables us to move from the laboratory experimental phase to that of prototype-scale design. The results of the three mathematical model sare summarized in Table VI. They reveal isotherm model coefficients of determination ranging from 0.89 to 0.99 for the Freundlich model, from 0.94 to 0.99 for the Temkin model and 0.99 for the Langmuir model. This would indicate that the Langmuir and Temkin models could better describe this system. However, given the values of the correlation coefficients, all very close to unity, the Langmuir model would be the most suitable. Estevinho and al [39] studied the elimination of pentachlorophenol by sweet almond shells in the raw state and reached the same conclusion on the isotherm model.

TableVI: - Parameters of adsorption isotherms for AG42 on CAC30.

	Langmuir constants			Freundlich constants			Temkin constants		
	Qm(mg/g)	b (L/mg)	R ²	Kf	1/n	R ²	KT (L/mg)	bT(J/mol)	R ²
30°C	3,01	0,16	0,99	0,85	0,33	0,89	1,99	1889,86	0,94
35°C	2,42	0,07	0,99	0,65	0,39	0,91	0,79	2022,45	0,95
40°C	2,76	0,02	0,99	0,45	0,53	0,98	0,51	1853,60	0,99
45°C	2,14	0,01	0,99	0,33	0,64	0,99	0,40	1757,36	0,97
50°C	2,11	0,01	0,99	0,35	0,57	0,96	0,44	2471,93	0,99

Thermodynamic parameters

The thermodynamic parameters of the adsorption process of AG42 on CAC30, the variation of the standard enthalpy ΔH° , the standard entropy ΔS° and the standard free enthalpy ΔG° were determined by implementing adsorption at five different temperatures (30, 35, 40, 45 and 50°C). The values of the thermodynamic parameters (ΔG° , ΔH° and ΔS°) derived from curve operation (variation of $\ln K_d$ as a function of $1/T$) are presented in Table VII. The ΔG° values calculated are negative, indicating that the adsorption process is spontaneous. The negative value of ΔH° reveals an exothermic, physical process [40]. The value $\Delta S^\circ < 0$ suggests a decrease in disorder at the adsorbent/solute interface [41].

TableVII: - Thermodynamic parameters (ΔG° , ΔH° and ΔS°).

T °C	ΔG° (KJ/mol)					ΔH° (KJ/mol)	ΔS° (KJ/mol)
	30°C	35°C	40°C	45°C	50°C		
CAC30	-11,31	-10,21	-9,11	-8,00	-6,90	-78,19	-0,22

Conclusion:-

The aim of our work was to evaluate the possibility of using hen eggshells as a high- performance activated carbon for the removal of the anionic dye AG 42, frequently used in textile dyeing, in particular modified acrylic fibers (nylon, polyamide) and animal fibers (wool and silk). We chose to prepare activated carbon chemically in the presence of phosphoric acid. Before studying the possibility of eliminating AG42 from aqueous solution, by adsorption onto the prepared activated carbon, we determined the latter's characteristics in order to elucidate the mechanisms of the phenomena involved. Generally speaking, the physico-chemical characteristics of the prepared activated carbon reveal that charcoal derived from hens' eggshells has a basic character and a small specific surface area of 5.42 m²/g, dominated by microporosity (3.56 m² /g).

Adsorption tests were used to establish the affinity between activated carbon and the dye (AG 42) in order to optimize its removal. The influence of adsorbent dose, pH, initial concentration and temperature was studied. In the experiments, an increase in the amount of AG42 adsorbed was observed with increasing activated carbon dose and initial dye concentration, up to a limit value of 30 g/L. Increasing pH and temperature reduces the binding capacity of AG42 to CAC30.

The pseudo-second-order model best describes the adsorption process of AG42 on CAC30, with coefficients of determination R² equal to 0.99. Three isotherm models were used to describe the adsorption isotherm of AG42 on CAC30. The results showed that adsorption on charcoal derived from hens' eggshells follows the Langmuir model, which has coefficients of determination R² ≥ 0.99.

The results of the thermodynamic study showed the spontaneous ($\Delta G < 0$) and exothermic ($\Delta H < 0$) nature of dye adsorption, with a well-organized distribution of dye molecules at the adsorption sites ($\Delta S^\circ < 0$)

References:-

- Kandisa R. V., Narayana S. K. V., Gopinadh R., Veerabhadramravi K. (2018).** Kinetic studies on adsorption of methylene blue using natural low-cost adsorbent. Journal of Industrial Pollution Control, vol. 34, No. 2, 2054-2058.
- Daghrir R., Drogui P. (2013).** Tetracycline antibiotics in the environment: a review. Environmental Chemistry Letters, vol. 11, No. 3, 209-227.
- Pearce C. I., Lloyd, Guthrie J. T. (2003).** The removal of colour from textile wastewater using whole bacterial cells: A review. Dyes and Pigments, vol. 58, No. 3, 179-196.
- Maurya M. S., Mittal A. K., Correl P. (2008).** Evaluation of adsorption potential of adsorbents: A case of up take of cationic dyes. Journal of Environment Biology, vol.29, 31-36.
- Vanessa P., Andrin A., Le Behec M., Lacombe S., Frayret J., Pigot T. (2017).** Photocatalysis-ferrate (VI) oxidation coupling for rhodamine 6G dye treatment. Revue des Sciences de l'Eau, vol. 30, 35-39.
- Tan I. A. W., Ahmad A. L., Hameed B. H. (2008).** Optimization of preparation conditions for activated carbons from coconut husk using response surface methodology. Journal of Chemical Engineering, vol. 136, 164-172.
- Kouadio D. L., Diarra M., Djassou A. C., Dibi B., Dongui B. K., Koné M., Traoré K. S., (2022).** Experimental study of blue 16 and red methyl adsorption on charcoal from cocoa pod shell. Journal de la Société Ouest-Africaine de Chimie, vol. 051, 17-30.
- Darmograi G., Prelot B., Layrac G., Tichit D., Martin-Gassin G., Salles F., Zajac J., (2015).** Study of adsorption and intercalation of orange-type dyes into Mg-Al layered double hydroxide. Journal of Physical Chemistry, vol. 119, 23388-23397.

9. **Dias J. (2007)**. Waste materials for activated carbon preparation and its use in aqueous-phase treatment: A review. *Journal of Environmental Management*, vol. 4, 833-846.
10. **Sanogo D., Aboua K. N., Soro D. B., Meite L., Kouadio D. L., Diarra M., Ehouman A. G. S., Traore K. S., Dembele A. (2020)**. Adsorption of Acid Green 42 in aqueous solution on activated carbon derived from moringa pod hulls. *Journal of Chemical Biological and Physical Science*, vol. 10, No. 2, 211-220.
11. **Rager T., Geoffroy A., Hilfikera R., John M., Storeyb D. (2012)**. The crystalline state of methylene blue: azoo of hydrates. *Physical Chemistry Chemical Physics*, vol.14, 8074-8082.
12. **Boehm H. P. (1994)**. Chemical identification of surface groups. *Advance catalys*, vol. 16, 25-31.
13. **Khalfaoui A. D. (2012)**. Experimental study of the removal of organic and inorganic pollutants by adsorption on natural materials: application to orange and banana peels. PhD thesis. Université Mentouri, Algeria, 143p.
14. **Kifuaani K. M. A., Noki V. P., Ndelo D. P. J., Mukana W. M. D., Ekoko B. G., Ilinga L. B., Mukinayi M. J. (2012)**. Adsorption of quinine dihydrochloride on an expensive activated carbon based on sugarcane Bagasse impregnated with phosphoric acid. *International Journal of Biology and Chemical Sciences*, vol. 6, 1337-1359.
15. **Brunauer S., Emmet P., Teller E. (1938)**. The adsorption of gases in multimolecular layers. *Journal of American Chemical Society*, vol. 60, 309-319.
16. **Habeeb O. A., Yasin F. M., Danhassan U. A. (2014)**. Characterization and application of chicken eggshell as green adsorbents for removal of H₂S from wastewaters. *Journal of Environmental Science Toxicology and Food Technology*, vol. 8, 7-12.
17. **Eren E. (2008)**. Removal of copper ions by modified Unye clay. *Journal of Hazardous Materials*, vol. 159, 235-244.
18. **Mezerette C., Vergnet L. F. (1994)**. "The thermochemical route «In: ANONYME. Guide Biomasse Energie. Collection Etudes et Filières, 144-198.
19. **Crini G., Badot M. P., (2008)**. "Treatment and purification of polluted industrial waters: Procèdes membranaires, bioadsorption et oxydation chimique," Presses universitaires de Franche-Comté, 283-285.
20. **Mestre A. S., Pires J., Nogueira J. M. F., Carvalho A. P. (2011)**. Activated carbons for the adsorption of ibuprofen. *Carbon*, vol. 45, 1979-1988.
21. **Barrette E. P., Joyner L. G., Halenda P. P. (1951)**. The determination of pore volume and area distributions in porous substances. I. Computations from Nitrogen isotherms. *Journal of American Chemistry Society*, vol. 73, 373-380.
22. **Adinata D., WanDaud W. M. A., Aroua M. K. (2007)**. Preparation and characterization of activated carbon from palm shell by chemical activation with K₂CO₃. *Bioresource Technology*, vol. 98, 145-149.
23. **Elkady M. F., Ibrahim A. M., El-Latif M. M. (2011)**. Assessment of the adsorption kinetics, equilibrium and thermodynamic for the potential removal of reactive red dye using eggshell biocomposite beads. *Desalination*, vol. 278, 412-423.
24. **Ashjaraan A., Yazdanshenas M E., Rashidi A., Khajavi R., Rezaee A. (2012)**. Biosorption thermodynamic and kinetic of direct dye from aqueous solutions on bacterial cellulose. *African Journal Microbiology Research*, vol. 6, 1270-1278.
25. **Atheba G. P., Allou N. B., Dongui B. K., Kra D. O., Gbassi K. G., Trokourey A. (2015)**. Adsorption of butylparaben on activated carbon based on coconut husks from Côte d'Ivoire. *International Journal of Innovation and Scientific Research*, vol. 13, 530-541.
26. **Sakr F., Sennaoui A., Elouardi M., Tamimi M., Assabane A. (2015)**. Study of Methylene Blue adsorption on a cactus-based bio-material. *Journal of Materials and Environment Sciences*, vol. 6, 397- 406.
27. **Pengthamkeerati P., Satapanajaru T., Singchan O. (2008)**. Sorption of reactive dye from aqueous solution on biomass fly ash. *Journal of Hazardous Materials*, vol. 53, 1149-1156.
28. **Guendouz S. (2014)**. Biosorption of textile dyes, Solophenyl Scarlet BNLE and Cibacron Green by dry biomass of duckweed. PhD thesis, University of Annaba, Algeria, 153p.
29. **Zhanying Z., Moghaddam L., O'hara M. I., Doherty W. O. S. (2011)**. Congo Red adsorption by ball-milled sugar cane bagasse. *Chemical Engineering Journal*, vol.178, 122-128.
30. **Rida K., Bouraoui S., Hadnine S. (2013)**. Adsorption of methylene blue from aqueous solution by kaolin and zeolite. *Applied Clay Science*, vol. 84, 99-105.
31. **Hors K. Y., Chee J. M. C., Chong M. N., Jin B., Saint C., Poh P. E., Aryal R. (2016)**. Evaluation of physicochemical methods in enhancing the adsorption performance of natural zeolite as low cost adsorbent of methylene blue dye from wastewater. *Journal of Cleaner Production*, vol. 118, 197-209.
32. **Pathania D., Sharma S., Singh P. (2017)**. Removal of methylene blue by adsorption onto activated carbon developed from Ficus caricabast. *Arabian Journal of Chemistry*, vol.10, 1445-1451.
33. **Li Z., Jia Z., Ni T., Li S. (2017)**. Adsorption of methylene blue on natural cotton based flexible carbon fiber

- aerogels activated by novel air-limited carbonization method. *Journal of Molecular Liquids*, vol. 242, 747-756.
34. **Hu Z., Chen H., Ji F., Yuan S. (2010)**. Removal of Congo red from aqueous solution by cattail root. *Journal of Hazardous Materials*, vol. 173, 292-297.
 35. **Gupta V. K., Jain R., Malathi S., Nayak A. (2010)**. Adsorption-desorption studies of indigo carmine from industrial effluents by using deoiled mustard and its comparison with charcoal. *Journal of Colloid and Interface Science*, vol. 348, 628-633.
 36. **Estevinho B. N., Ratola N., Alves A., Santos L. (2006)**. Pentachlorophenol removal from aqueous matrices by sorption with almond shell residues. *Journal of Hazardous Materials*, vol. 137, 1175-1181.
 37. **Idris S. A. M. (2015)**. Adsorption, kinetic and thermodynamic studies for manganese extraction from aqueous medium using mesoporous silica. *Journal of Colloid and Interface Science*, vol. 440, 84-90.
 38. **Seghier A. (2018)**. Preparation and modification of a plant precursor for water treatment. PhD thesis, University of Oran, Algeria, 143p.
 39. **Rahman M., Adil M., Yusof A. M., Kamaruzzaman Y. B., Ansary R. H. (2014)**. Removal of Heavy Metal Ions with Acid Activated Carbons Derived from Oil Palm and Coconut Shells. *Journal of Hazardous Materials*, vol. 7, 3634-3650.
 40. **Ghaedi A. M., Ghaedi M., Vafaei A., Irvani N., Keshavarz M., Rad M., Tyagi I., Agarwal S., Gupta V. K. (2015)**. Adsorption of copper (II) using modified activated carbon prepared from Pomegranate wood: Optimization by bee algorithm and response surface methodology. *Journal of Molecular Liquids*, vol. 206, 195-206.
 41. **Boumchita S., Lahrichi A., Benjelloun Y., Lairini S., Nenov V., Zerrouq F. (2016)**. Removal of a cationic dye from an aqueous solution by a food waste: potato peel. *Journal of Mater and Environmental Sciences*, vol. 7, 73.